Least Squares Method Identification of Corona Current-Voltage Characteristics and Electromagnetic Field in Electrostatic Precipitator

H. Nouri, I. E. Achouri, A. Grimes, H. Ait Said, M. Aissou, Y. Zebboudj

Abstract—This paper aims to analysis the behavior of DC corona discharge in wire-to-plate electrostatic precipitators (ESP). Current-voltage curves are particularly analyzed. Experimental results show that discharge current is strongly affected by the applied voltage.

The proposed method of current identification is to use the method of least squares. Least squares problems that of into two categories: linear or ordinary least squares and non-linear least squares, depending on whether or not the residuals are linear in all unknowns. The linear least-squares problem occurs in statistical regression analysis; it has a closed-form solution. A closed-form solution (or closed form expression) is any formula that can be evaluated in a finite number of standard operations. The non-linear problem has no closed-form solution and is usually solved by iterative.

Keywords—Electrostatic precipitator, current-voltage characteristics, Least Squares method, electric field, magnetic field.

I. INTRODUCTION

THE Electrostatic Precipitators (ESP) are used with success to reduce the emissions of smoke, fumes and dust, playing an important role to maintain a clean environment and to improve the air quality [1]. They are able to remove more than 99% of the particulates from the flue gas in terms of mass [2]. In these systems, particles are typically charged by the ions produced by a DC corona discharge. AC or dielectric barrier discharges are also efficient if the appropriate frequency is used [3]. The electrically charged particles are then driven by the Coulomb forces due to the electric field present in the inter-electrode gap. Their migration towards the collecting electrodes is also affected by the viscous forces associated with the fluid flow and the ionic wind [4]–[7].

The major difference between wet and dry ESPs is that the charged particles, on arriving at the collecting electrodes, are removed by a flushing liquid (usually water) instead of mechanical rapping [8], [9]. In the case of humid gases, sticky or low electrical resistivity particles, wet ESP are used with success to control fine particle emissions [10], [11]. Some aspects of this effect require further investigations in order to validate a realistic mathematical model of the physical phenomena, as an essential step towards the accurate numerical simulation of the electrostatic precipitation process.

The main objective of this investigation is to quantify the model parameters effect in the ESP performance Process Dynamics and Control: Modeling for Control and Prediction is a comprehensive introduction to the subject divided in the broad parts. The first part deals with building physical models, the second part with developing empirical models and the final part discusses developing process control solutions. The paper takes an approach to the subject by looking at both physical and empirical modeling.

System identification is an important approach to model dynamical systems and has been used in many areas such as chemical processes, and electrical engineering. Several methods have been developed for system identification, e.g., the least squares methods, gradient based methods, the maximum likelihood methods, and the step response based method. Some useful techniques are used in system identification [12]-[14].

The term least squares describes a frequently used approach to solving over determined or inexactly specified systems of equations in an approximate sense. Instead of solving the equations exactly, we seek only to minimize the sum of the squares of the residuals. The least squares criterion has important statistical interpretations. If appropriate probabilistic assumptions about underlying error distributions are made, least squares produces what is known as the maximum-likelihood estimate of the parameters. Even if the probabilistic assumptions are not satisfied, years of experience have shown that least squares produce useful results.

The computational techniques for linear least squares problems make use of orthogonal matrix factorizations.

II. EXPERIMENTAL SETUP

To lead our experimental study, we have achieved wires - plates system of electrodes, as shown in Fig. 1.

The ESP based on a DC corona, consists of two parallel electrodes (stainless steel plates, 200-mm-length and 100-mm-width in x-direction and z- direction, respectively). Both parallel electrodes are grounded. The high voltage electrodes consist of a stainless steel wires with different diameters (0.2, 0.3, 0.41, 0.61 and 0.81 mm) parallel to z-axis midway between the grounded electrodes. The distance between both grounded plates is equal to 100 mm.

H. Nouri, I. E. Achouri and A. Grime are with the Department of Electrical Engineering, Seif_1 University, 19000 Algeria (Corresponding author: H. Nouri, phone: 213-772-531-073; fax: 213-366-112; e-mail: nouri_hamou@yahoo.fr, atabbel@yahoo.fr, atabbel@yahoo.fr).).

H. Ait Said, M. Aissou and Y. Zebboudj are with the Department of Electrical Engineering, Bejaia University, 06000 Algeria (e-mail: hakimdoz@yahoo.fr, aissoumas@yahoo.fr, yzebboudj@yahoo.fr).

World Academy of Science, Engineering and Technology
International Journal of Electrical and Computer Engineering
Vol:9, No:12, 2015

Fig. 1 Experimental setup

The schematic representations of the wire-to-plane ESP used in this investigation are shown in Fig. 2. In the first ESP (called 1W-ESP, Fig. 2 (a)), only one wire is connected to the high voltage. However, the second configuration (called 2W-ESP, Fig. 2 (b)) uses 2 similar wires. The distance between two successive wires is set to 40 mm or 80mm. The third configuration (called 3W-ESP, Fig. 2 (c)) uses 3 similar wires to create the corona discharges. The distance between two successive wires is set to 40 mm.

In this study, the two DC high voltage polarities were used (positive and negative). The high voltage was applied by a DC power supply (SPELLMAN SL 150, $\pm$ 40 kV; $\pm$3.75 mA) with an accuracy of 0.1 kV. The power supply was protected by a ballast resistor of 10kΩ. The time-averaged current was measured using a digital millimeter (METERMAN 37 XR, accuracy $\approx$1μA)

The current-voltage curves represent the average of three series of measurements.

III. PROPOSED METHOD OF ANALYSIS

The method of least squares assumes that the best-fit curve of a given type is the curve that has the minimal sum of the deviations squared (least square error) from a given set of data [15], [16].

Suppose that the data points are (x_1,y_1), (x_2,y_2), ..., (x_n,y_n) where x is the independent variable and y is the dependent variable. The fitting curve f(x) has the deviation (error) d from each data point:

$$\begin{cases} d_1 = y_1 - f(x_1) \\ d_2 = y_2 - f(x_2) \\ \cdots\cdots \cdots\cdots \cdots \\ d_n = y_n - f(x_n) \end{cases} \quad (1)$$

According to the method of least squares, the best fitting curve has the property that:

$$\sum_{i=1}^{n} d_i^2 = \sum_{i=1}^{n} \left[y_i - f(x_i) \right]^2 = \text{Minimum} \quad (2)$$

(a)

(b)

(c)

Fig. 2 Laboratory ESP configurations: (a) 1W-ESP, (b) 2W-ESP and (b) 3W-ESP

A. Algorithm of Least Squares Method (Linear Models)

Perform a set of n measurements of input and output of the process. The n sets being given (with their weight w_i) [15].

1. Propose a model in other words define the functions component model:

$$y_i^* = \sum_{j=1}^{m} c_j f_j(x_i) \quad (3)$$

World Academy of Science, Engineering and Technology
International Journal of Electrical and Computer Engineering
Vol:9, No:12, 2015

2. Calculate the terms:

$$a_{kj} = \sum_{i=1}^{n} f_j(x_i) f_k(x_i) w_i \quad k= 1, m; \; j= 1,m \qquad (4)$$

$$b_k = \sum_{i=1}^{n} w_i y_i f_k(x_i) \qquad (5)$$

3. Solve the linear system symmetric matrix:

$$\sum_{j=1}^{m} a_{kj} c_j = b_k \qquad (6)$$

B. Quality Measuring of an Approximation

When we approximate a set of numerical data $\{y(x_i)/i=1,n\}$ by an analytic function $y^*(x_i)$, which is to make a good approximation. We believe that $y - y^*$ must be small in some sense. The distance between the real function y and its model y^* can be measured by the least-square norm.

$$\|y - y^*\|_{2,w} = \sum_{i=1}^{n} (y_i - y_i^*)^2 w_i; w \geq 0; i=1,n. \qquad (7)$$

The error committed at point i by approximating the measured by is written as:

$$e_i = y_i - y_i^* = y_i - \sum_{j=1}^{m} c_j f_j(x_i) \qquad (8)$$

This system of n equations at unknown (n+m) ($c_j; j=1,m; e_i=1,n$) has infinitely many solutions. Among these solutions, we use define that with supers making minimum quality scalar;

$$Z = \sum_{i=1}^{n} e_i^2 w_i \qquad (9)$$

It aims to minimize Z by setting the parameter value ($c_1,...,c_m$) in a condition that:

$$\frac{\partial Z}{\partial c_k} = 0 : \text{is a linear system to solve} \qquad (10)$$

IV. RESULTS AND DISCUSSION

A. The Current-Voltage Characteristics

All measurements were made in an air-conditioned laboratory, where the temperature was maintained at 22°C, the pressure was maintained at 750 torr and relative humidity was maintained at 50% (The physical parameters of air are regularly controlled).

Figs. 3 and 4 show the current-voltage characteristics obtained with the ESP for both voltage polarities. Obviously, the discharge current increases gradually as the applied voltage increases. In addition, the discharge current is higher

with negative polarity for a given voltage, which is due to the difference in apparent mobility of charge carriers [9]. This phenomenon is attributed to the fact that in the cathode corona case higher electron emission and faster formation of avalanches.

This section is used to investigate the effect of corona wire radius on the ESP current voltage characteristics. The results indicate that better current is obtained with thinner corona wires under the same average electric field (or applied voltage). Similar discharge behavior is observed in the case of 1W-ESP, 2W-ESP, and 3W-ESP. However, current magnitude with three wires is lower than three times the current magnitude with one wire:

$$\begin{cases} I_{1wire} < I_{3wires} < 3 \times I_{1wire} \\ I_{1wire} < I_{2wires} < 2 \times I_{1wire} \\ I_{2wires} < I_{3wires} < \dfrac{3}{2} \times I_{2wires} \end{cases} \qquad (11)$$

This is due to the electric field interaction between two successive high voltage wires. In fact, the distance between the wires is lower than the interelectrode gap.

B. Corona Onset Voltage

Fig. 5 shows the evolution of V_s against the wires radius for both high voltage polarities. The time-averaged discharge current, which crosses the inter electrode gap is a non-linear function of the applied voltage.

The voltage necessary to overcome this critical field strength, however, is set by the complete configuration of discharge and collecting electrodes.

We can observe that corona onset voltage is higher in the case of 3W-ESP and especially for negative polarity. Whatever the case, V_s increases with the electrode diameters.

C. Procedure to Determine the Best Fit Line to Data

For this part we will consider only the case for the 1W-ESP. The basic problem is to find the bestfit $y_M = \sum_{i=1}^{m} c_i f_i(x)$ given that, for $m \in \{1,....,n\}$, the pairs (x$_n$; y$_n$) are observed. Tables I and II show the different parameters calculated by least squares method [15]:

$$S^2 = \frac{e^t e}{n-m} : \text{is the estimator of the variance } \sigma \qquad (12)$$

$$\sigma = \frac{1}{n} \sum_{i=1}^{n} e_i^2 \qquad (13)$$

$$e = y_{\text{exp}\,erementale} \_ y_m : \text{Error vector} \qquad (14)$$

$$z = e^t w e_i : \text{modeling error} \qquad (15)$$

In addition, w: weighting ($0 \leq w \leq 1$).

World Academy of Science, Engineering and Technology
International Journal of Electrical and Computer Engineering
Vol:9, No:12, 2015

TABLE I
INFLUENCE OF ORDER ON THE ERROR (POSITIVE CORONA)

m	z	S^2
2	1.6279×10^{-8}	1.0174×10^{-9}
3	1.2149×10^{-10}	8.00993×10^{-11}
4	3.4607×10^{-11}	2.4719×10^{-12}
5	2.27879×10^{-11}	2.1446×10^{-12}

TABLE II
INFLUENCE OF ORDER ON THE ERROR (NEGATIVE CORONA)

m	z	S^2
2	2.4815×10^{-8}	1.5509×10^{-9}
3	1.5398×10^{-10}	1.0265×10^{-11}
4	7.1211×10^{-11}	5.0865×10^{-12}
5	6.0873×10^{-11}	4.6825×10^{-12}

Variations the model and experimental result are shown in Figs. 6 and 7.

We find that the process stabilizes, so we can use the model to $3 \leq m \leq 5$:

− *Positive corona*:

$$I_{mP} = \text{« } 2.7159 \times 10^{-5} - 5.8841 \times 10^{-9} \, V + 2.5593 \times 10^{13} \, V^2 + 4.8248 \times 10^{-18} \, V^3 - 8.0126 \times 10^{-23} \, V^4 \text{ »}$$

− *Negative corona:*

$$I_{mN} = \text{« } 3.34 \times 10^{-5} - 6.91 \times 10^{-9} \, V + 2.69 \times 10^{-9} \, V^2 + 6.65 \times 10^{-18} \, V^3 - 9.93 \times 10^{-23} \, V^4 \text{ »}$$

D. Corona Onset Field Strength

Using the onset potential VS we found by drawing the current–voltage I = f(V) characteristic, E0 can be calculated as [17]:

$$E_0 = \frac{V_S}{h \ln(R / r_0)} \qquad (16)$$

where r_0 is the conductor radius in centimeters, h is the distance between the wire and the collector plate and R is the equivalent radius.

Fig. 8 shows the onset electric field curves in the case of one wire- two plates electrostatic precipitator for both high voltage polarities.

Fig. 4 Current-voltage characteristic of negative corona
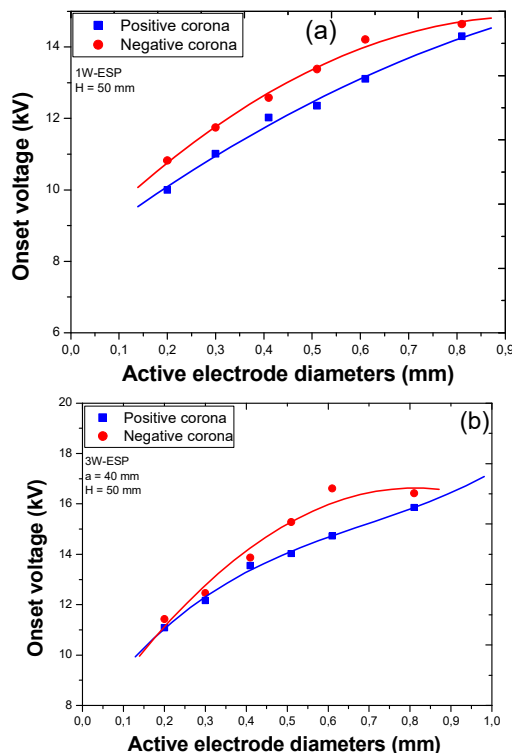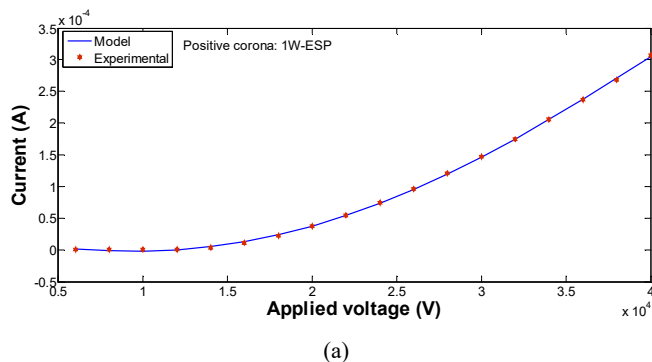

Fig. 5 Variation of corona onset voltage with active electrode diameters: (a) Positive corona and (b) Negative corona one wire- two plates electrostatic precipitator for both high voltage polarities
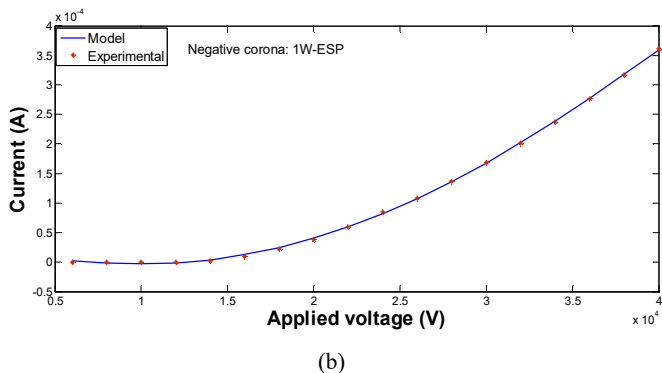

Fig. 3 Current-voltage characteristic of positive corona

(a)

World Academy of Science, Engineering and Technology
International Journal of Electrical and Computer Engineering
Vol:9, No:12, 2015

(b)

Fig. 6 Comparison of model with experimental: (a) Positive corona and (b) Negative corona

E. The Magnetic Field Generated

The magnetic field of an electric line is generated only from the current flow. A simple application of Ampere's law is used to calculate the value of the magnetic field around a simple conductor.

To calculate the magnetic field at the ground in the vicinity of an energy transport line, a long electric wire carrying an electric current is considered.

The conductors are cylindrical, the radius of the conductors is small compared to its length, and its height above the plane is placed on the surface ground [18], [19].

$$\vec{H} = \frac{\vec{I}}{2.\pi.r} \quad (17)$$

The magnetic induction is given by:

$$\vec{B} = \mu \, \vec{H} \quad (18)$$

where μ is the magnetic permeability.

For our case and for any triangle (Fig. 9), we can write the distribution in terms of magnetic field as a function only of the variables x and y:

$$\vec{B} = \frac{\mu_0 \, \vec{I}}{2.\pi.r} = \frac{\mu_0 . \vec{I}}{2\pi \sqrt{h^2 + x^2}} \quad (19)$$

Immediately adjacent to the ground, the magnetic field data is shown in Fig. 10.

It is found that around a circular area with a radius of about 2 cm below the center line of the wire at a height of 5 cm, the magnetic field has a significant value and can cause problems for living beings and electronic devices. It is also noted that when the field source has a simple geometry, such as a power line, it is relatively easy to predict the levels of electric and magnetic field in its vicinity.

IV. CONCLUSION

In this paper, the effect of geometry on a dc corona discharge behavior in wire-to-plane electrostatic precipitator has been discussed. Several design parameters have been taken into consideration especially the numbers of active electrodes and their diameter.

The electrostatic precipitator current voltage is identified by least squares method. The comparison of the experimental and numerical values confirms the convenience of the identification method.

Corona onset voltage, which is higher with three wires construction and thicker ones, increases with increasing the diameters of wires. The electric field and magnetic field are inversely proportional to the increase of distance.
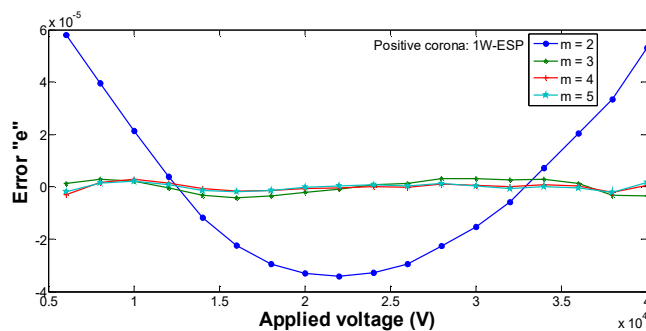
(a)
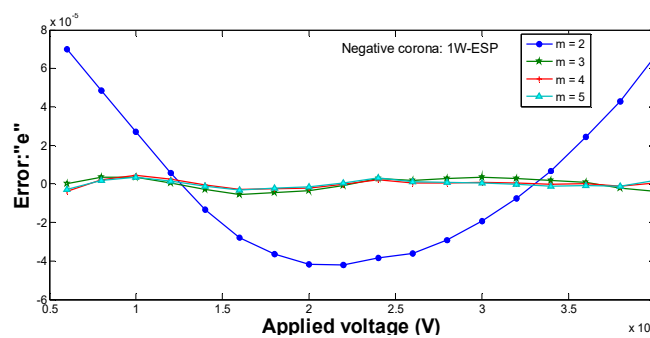
(b)

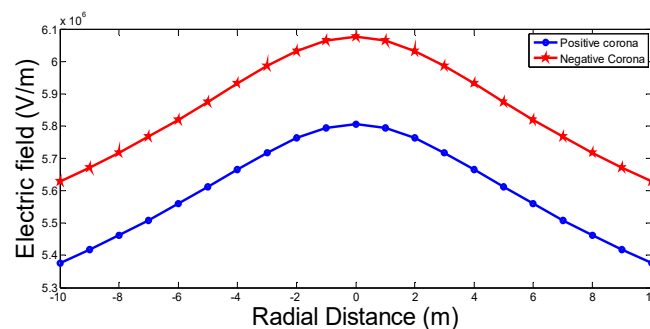Fig. 7 Influence of order m on the error: (a) Positive corona and (b) Negative corona

Fig. 8 Variation of corona onset field strength

World Academy of Science, Engineering and Technology
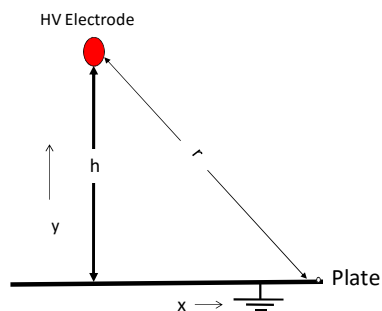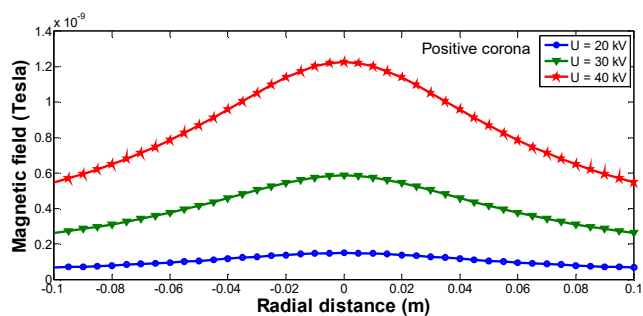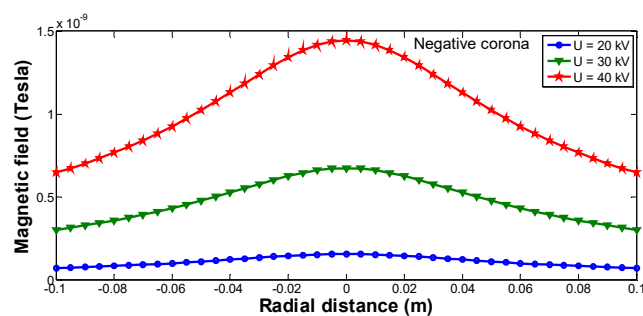International Journal of Electrical and Computer Engineering
Vol:9, No:12, 2015

Fig. 9 Configuration of electrodes (triangle)

(a)

(b)

Fig. 10 Variation of corona magnetic field: (a) Positive corona and (b) Negative corona

REFERENCES

[1] A. Mizuno, Electrostatic precipitation, *IEEE Trans. Dielectr. Electr. Insul.* 7, pp. 615-624, 2000.
[2] J. S. Chang, Next generation integrated electrostatic gas cleaning systems, *J. Electrostat.* 57, pp. 273-291, 2003.
[3] T. Yamamoto and H. R. Velkoff, Electrohydrodynamics in an electrostatic precipitator, *J. Fluid Mech.* 108, pp. 1–18, 1981
[4] P. Atten, F. M. J. Mccluskey and A. C. Lahjomri, The electrohydrodynamic origin of turbulence in electrostatic precipitators, *IEEE Trans. Ind. Appl*, 23, pp. 705–711, 1987.
[5] J. Podliński, J. Dekowski, J. Mizeraczyk, D. Brocilo and J. S. Chang, Electrohydrodynamic gas flow in a positive polarity wire-plate electrostatic precipitator and the related dust particle collection efficiency, *J. Electrostatic.* 64, pp.259-262, 2006.
[6] N. Zouzou, B. Dramane, P. Braud, E. Moreau and G. Touchard, EHD flow in DBD precipitator, *IJPEST*, 3, pp.142-145, 2009.
[7] H. Nouri, N. Zouzou, E. Moreau, L. Dascalescu, Y. Zebboudj, Effect of relative humidity on the collection efficiency of a wire-to-plane electrostatic precipitator, *The IEEE Industry Applications Society Annual Meeting*, Houston, Tx, ISSN: 0197-2618, Print ISBN: 978-1-4244-6393-0 3-7 October, 2010.
[8] K. R. Parker, Applied Electrostatic Precipitation, *Edition Kluwer Academic Publishers*, London, 1997.
[9] H. Nouri, N. Zouzou, E. Mreau, L. Dascalescu, Y. Zebboudj, Effect of Relative Humidity on Current-Voltage Characteristics of an Electrostatic Precipitator, *Journal of Electrostatics*, 2012, Vol 70 N° 1, pp. 20-24, 2012.
[10] H. Nouri and Y. Zebboudj, Analysis of Positive Corona in Wire-to-Plate Electrostatic Precipitator, *Eur. Phys. J. Appl. Phys*., Vol. 49,p 11001, 2010.
[11] A. Bologa, H. R. Paur, H. Seifert, Th. Wäscher and K. Woletz, Novel wet electrostatic precipitator for collection of fine aerosol, *J. Electrostatics*. 67, pp.150–153, 2009.
[12] P. Joaquim, S. Marques, Applied Statistics Using SPSS, STATISTICA, MATLAB and R. *Springer-Verlag Berlin Heidelberg*, Second Edition, pp. 271- 327, 2007.
[13] D. Alexander, Z. Poularikas, M. Ramadan, Adaptive filtering primer with matlab. *CRC Press Taylor & Francis Group*, pp. 101 - 197, 2006.
[14] F. van der Heijden, R .P. W. Duin, D. de Ridder, D. M. J. Tax, Classification, Parameter Estimation and State Estimation An Engineering Approach using MATLAB, *John Wiley & Sons Ltd, The Atrium, Southern Gate*, Chichester, West Sussex PO19 8SQ, England, pp. 13 -138, 2004.
[15] M. Boumahrat, A.Gourdin, Méthodes numériques appliquée, *OPU*, pp. 293 – 364, 1993.
[16] P. Borne, Modélisation et identification des processus, Tome 2, *Editions Technip*, Paris, France, 1992.
[17] M. Abdel– Salam, Z. Al– Hamouz, Analysis of monopolar ionized field as influenced by ion diffusion, *IEEE Trans., Ind. App*, vol.31, pp.484-493, 1995.
[18] S. Pasare, calcul de champ magnétique d'une ligne aérienne a haute tension, *Electrical engineering series*, N°:32, 2008.
[19] M. Nicolas, Ondes et électromagnétisme, *Dunod*, Paris, ISBN 978-2-10-054276-5, pp.133- 159, 2009.

Hamou Nouri was born in Algeria. He received the Ph.D degree in electrical engineering, from Bejaia University, Algeria in 2010 and then the "Habilitation à Diriger de Recherches" diploma in electrical engineering in 2012. He is currently associate professor in the department of electrical engineering, Setif University. His research interests are the application of corona discharge, non – thermal plasma technology and air pollution control. His major interests are in the mathematical modelling of electrostatics systems. Dr. Nouri is a member of Laboratoire de Génie Electrique of the University A. Mira of Bejaia. and French society of electrostatics.